JMEPEG (2011) 20:231–237
DOI: 10.1007/s11665-010-9678-1

1059-9495/$19.00

A Study on Microstructure and Dielectric Performances of Alumina/Copper Composites by Plasma Spray Coating

Kuan Hong Lin, Zi Hao Xu, and Shun Tian Lin

(Submitted September 25, 2009)

In this study, surfaces of copper plates were coated with a thick alumina layer by the plasma spray coating to fabricate a composite with a dielectric performance that made them suitable as substrates in electronic devices with high thermal dissipation. The performance of alumina dielectric layer fabricated by the plasma spray coating and traditional screen-printing process was compared, respectively. Effects of the spraying parameters and size of alumina particles on the microstructure, thickness, and the surface roughness of the coated layer were explored. In addition, the thermal resistance perpendicular to the interface of copper and alumina and the breakdown voltage across the alumina layer of the composite were also investigated. Experimental results indicated that alumina particles with 5-22 μm in diameter tended to form a thicker layer with a poorer surface roughness than that of the particles with 22-45 μm in diameter. The thermal resistance increased with the surface roughness of the alumina layer, and the breakdown voltage was affected by the ambient moisture, the microstructure and the thickness of the layer. The optimal parameters for plasma spray coating were an alumina powder of particles size between 22 and 45 μm, a plasma power of 40 kW, a spraying velocity of 750 m/s, an argon flow rate of 45 L/min, a spraying distance of 140 mm, and a spraying angle of 90°. It can be concluded that an alumina layer thickness of 20 μm provided a low surface roughness, low thermal resistance, and highly reliable breakdown voltage (38 V/μm).

Keywords alumina, composite, dielectric, plasma spray coating, thermal resistance

1. Introduction

The thermal energy dissipated by a microelectronic component is conducted first from the component to the surface of the dielectric layer, from which the thermal energy is subsequently conducted through the dielectric substrate and finally removed by convection in a heat sink. In most cases, the high thermal resistance of the dielectric layer, such as an epoxy-ceramic composite, obstructs heat transfer from the interior of the component to the surface of the heat sink, even when an auxiliary heat dissipation device is adopted.

The poor heat dissipation ability of a traditional printed circuit board (PCB, thermal conductivity $k = 0.3$ W/m K) (Ref 1) is not satisfactory for the high-power electronic components. Accordingly, researchers have developed metal-core printed circuit boards (MCPCB) (Ref 2) and insulated metal substrate (IMS) (Ref 3-5) to improve the heat dissipation of PCB. An MCPCB is attached with a high-thermal spreading metal, such as aluminum or copper to promote heat dissipation effectively by an increase of k from 1 to 2.2 W/m K (Ref 2). Thus, the heat dissipation performance of the MCPCB is better than that of a traditional PCB. However, a dielectric layer that consists of epoxy polymer and inorganic powder has a low thermal conductivity ($k = 0.36$ W/m K) (Ref 6), which results in an inefficient heat dissipation in a traditional MCPCB. The process in the fabrication of an IMS is an assembly of a polymer insulating layer and a copper circuit on an aluminum or copper substrate. The thermal conductivity of such an insulated layer is about 1.1-2 W/m K (Ref 3-5), which exceeds that of the PCB by a factor of three to six. However, the thickness of the insulated layer dominates the thermal conduction performance of the IMS. A thicker insulated-layer provides a higher thermal resistance and a lower thermal conductivity, whereas an insufficient thickness causes electric leakage and a short circuit.

The plasma spray coating of ceramic powder onto a copper substrate to fabricate a layered composite may mitigate aforementioned issues. The ceramic powder used in plasma spray coating should not sublimate or decompose at high temperature. Ceramic powders that have a high thermal conductivity; high electrical insulation, and spherical particles of sizes between 5 and 100 μm are preferred. Table 1 presents the physical properties of ceramic powders used in plasma spray coating (Ref 7). The thermal conductivity of Al_2O_3 powder ($k = 30$ W/m K) is lower than that of AlN or SiC; however, its easy production and lower cost make it suitable for use in the dielectric layers of high-power electric devices.

In this study, pure alumina powders of two particle sizes were coated onto the copper substrate by plasma spray coating. The thickness of the alumina dielectric layer was controlled <40 μm. The dielectric layer with low thermal resistance, high electric insulation, less porosity, and an ideal microstructure will be expected. Subsequently, the heat dissipation performance of an alumina dielectric layer fabricated by plasma spray coating will be compared with that of the traditional screen-printed alumina thermal pad. The optimal working parameters

Kuan Hong Lin, Department of Mechanical Engineering, Tungnan University, Taipei, Taiwan; and **Zi Hao Xu** and **Shun Tian Lin**, Department of Mechanical Engineering, National Taiwan University of Science and Technology, Taipei, Taiwan. Contact e-mail: khlin@mail.tnu.edu.tw.

to produce a plasma spray coating with improved heat dissipation performance were proposed in this study.

2. Experimental Procedures

The surface of a copper substrate was coated with an alumina dielectric layer to fabricate an alumina/copper-layered composite by screen-printing and plasma spray coating, respectively. The screen-printing process involved the mixing of alumina powders (50 vol.%) and styrene-butadiene rubber (SBR) solution into a paste. Subsequently, a screen device was used to transfer the paste onto a copper substrate by controlling the position of the screen to yield the required thickness. Finally, alumina thermal pad/copper composites with thickness values of 200 and 250 μm were formed, respectively. Table 2 presents the experimental conditions of the screen-printed alumina thermal pad/copper composites. On the other hand, the surface of the copper substrate was grit-blasted before it was plasma spray-coated. The constant working parameters of the plasma spray coating were a spraying velocity of 750 m/s, an argon flow rate of 45 L/min, a spraying distance of 140 mm, and a spraying angle of 90°. The varied parameters and the specimen designation number are shown in Table 3.

The cross-sectional images of the plasma spray-coated alumina/copper composites were recorded using a field emission scanning electron microscope (FESEM, JEOL, JSM-6500F). The corresponding mapping of aluminum, copper and oxygen elements of the composites were examined using an energy-dispersive spectrometer (EDS, OXFORD, INCA Energy 300). The crystalline structure of the composites was analyzed using an x-ray diffractometer (XRD, REGAKU, DMAX-VB) at 40 kV and 100 mA, using Cu K_α ($\lambda = 0.15418$ nm) radiation. The surface roughness of the alumina layer formed by plasma spray coating was measured using a surface roughness tester (HOMMELWERKE, LV-50E). The thermal resistance perpendicular to the interface of the alumina layer (or alumina thermal pad) and copper substrate was measured using a thermal interface material tester (LONG WIN SCIENCE, LW-9091), over a test area 0.0254 m × 0.0254 m, at a clamp pressure of 8 kgf, and with input powers of 80 W. The structure for recording the thermal resistance of the composite was in the form, thermally conducting grease-alumina layer-copper-thermally conducting grease. Although it was a sandwich-like structure, it can be regarded as a one-dimensional structure for heat transfer. Therefore, the thermal resistance of the alumina layer can be expressed as,

$$R_{Al_2O_3} = R_{Real}\text{-}R_{Cu}\text{-}R_{Thermalgrease}\text{-}R_{Background},$$

where R_{Real} is the measured thermal resistance; R_{Cu} is the thermal resistance of copper; $R_{Thermal\ grease}$ is the thermal resistance of thermally conducting grease, and $R_{Background}$ is the background noise, which was assumed to be the same in all tests.

The electrical resistivity (ρ) values of the layered alumina and the alumina thermal pad were measured respectively, using a four-point probe resistivity measurement tester (KEITHLEY, 2400) with a maximum measurement limit of 10^{14} Ω cm. The mean value among five measuring points was recorded for each specimen. A puncture and insulation tester (TOPWARD, TPT-500) was used to measure the breakdown voltage of the alumina layer and alumina thermal pad produced by various processing parameters. The effect of ambient moisture on the breakdown voltage of the alumina layer was also determined.

Table 1 Physical properties of ceramic powders used in plasma spray coating (Ref 7)

Properties	Al_2O_3	AlN	SiC
Density, g/cm^3	3.98	3.26	3.2
Melting point, °C	2015	2230	2830
Thermal conductivity, W/m K	~30	~150	~250
Electric resistivity, Ω cm at RT	$>10^{14}$	$\sim10^{14}$	10^3-10^5

Table 2 Experimental conditions of screen-printing of alumina thermal pad/copper composites

Conditions	SBR	Al_2O_3
Density, g/cm^3	1.04	3.99
Particle size, μm	...	44
Filling percentage, vol.%	50	50
Weight percentage, wt.%	20.7	79.3
Thickness of Al_2O_3 thermal pad, μm	200	250
Specimen designation number	S200	S250

3. Results and Discussion

3.1 Screen-Printed Alumina Thermal Pad/Copper Composite

Figure 1 illustrates the thermal resistance of two screen-printed alumina thermal pads under 80 W input power. The thermal resistance of specimens S200 (thickness 200 μm) and S250 (thickness 250 μm) were 0.27 and 0.41 K/W, respectively. Clearly, as the thickness of the alumina thermal pad was increased by 25%, its thermal resistance increased by 52%. Furthermore, the thermal conductivity coefficient K decreased by 17% from 1.15 to 0.95 W/m K. It is reported that the screen-printing process is suitable for fabricating an alumina thermal pad with a thickness over 100 μm (Ref 8). The traditional screen-printing process cannot make the thermal pad sufficiently thin to yield a low-thermal resistance easily, due to cost and technical limitations. The excellent electric insulation of alumina powder and SBR, and the thickness of the alumina thermal pad exceeding 200 μm would cause the electrical

Table 3 Parameters of plasma spray coating and designation number of specimens in this test

Specimen designation number	A1	A2	A3	B1	B2	B3	C1	C2	C3	D1	D2	D3
Plasma power, kW	35.2	40	45	35.2	40	45	35.2	40	45	35.2	40	45
Layer thickness, μm	20	20	20	40	40	40	20	20	20	40	40	40
Particle size, μm	5-22	5-22	5-22	5-22	5-22	5-22	22-45	22-45	22-45	22-45	22-45	22-45

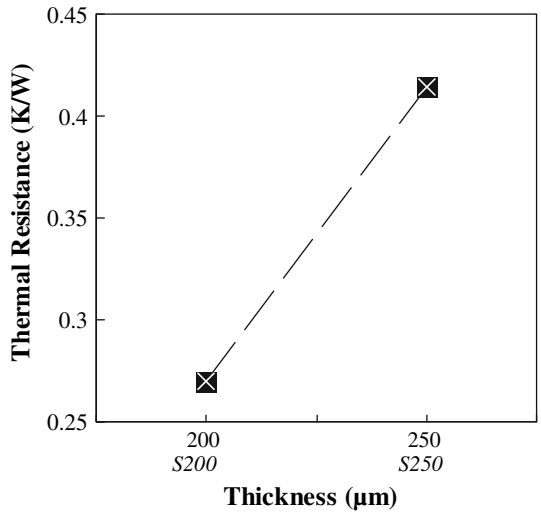

Fig. 1 Thermal resistance of two screen-printed alumina thermal pad subjected to 80 W input power; test area was 0.0254 m × 0.0254 m

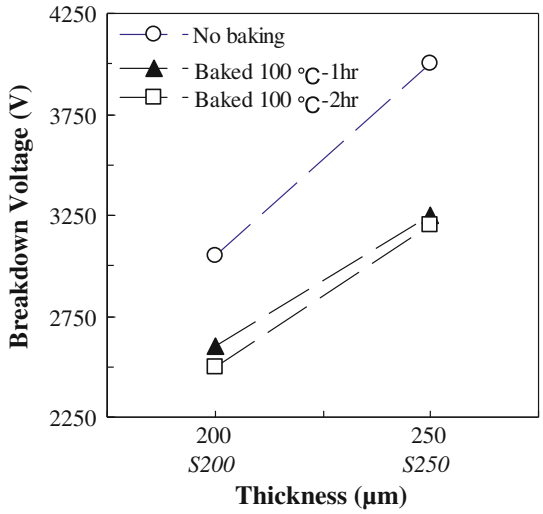

Fig. 2 Breakdown voltage of two screen-printed alumina thermal pad/copper composites before baking and baked at 100 °C for 1 and 2 h, respectively

resistivity of the two screen-printed alumina thermal pads higher than 10^{14} Ω cm.

The breakdown voltages of two screen-printed alumina thermal pad/copper composites are shown in Fig. 2, which were baked at 100 °C for 1 and 2 h, respectively. The breakdown voltage of the composites was expected to increase with the baking time, but contrary results were observed. The cross-sectional optical micrograph of the S250 specimen before baking is shown in Fig. 3(a). The spall phenomenon was observed after baking, implying air is presented between the alumina thermal pad and the copper substrate, as illustrated in Fig. 3(b). It can be attributed to the great difference between the thermal expansion coefficients of the alumina thermal pad and copper. The breakdown voltage of air (~3000 V/mm) (Ref 9) was much lower than that of the alumina thermal pad, and therefore reduced the breakdown voltage value of the composite.

3.2 Plasma Spray-Coated Alumina/Copper-Layered Composites

Figure 4 depicts the secondary electron images of all plasma spray-coated alumina/copper-layered composites. The region between the Cu and epoxy as indicated by arrows in Fig. 4(a) is alumina layer, which is bonded with the Cu substrate excellently in each specimen. However, the alumina layers in all specimens were porous. The porosity of the alumina layers increased with the thickness of the layer, which can be revealed by the comparison of C3 in Fig. 4(i) and D3 in Fig. 4(l). On the other hand, the porosity decreased with an increase of particle size, which can be observed on the A3 specimen in Fig. 4(c) and the C3 specimen in Fig. 4(i).

The mean thickness of the alumina layers in the specimen A1 was about 20 μm, which was very close to the original scheme. However, the layer thickness of specimen A3 was approximately 40 μm, exceeding the expected value by around 100%. Similar result was observed for specimen B3 as displayed in Fig. 4(f). The average thickness of the alumina layers in specimens C and D groups were very close to the expected values, with the exception of specimen C3 and D3, in which the thickness was about 20% higher, due to a higher spraying power (45 kW). The spraying power had a greater influence on the thickness of fine powder (5-22 μm) than that of the coarse powder (22- 45 μm). For a finer powder, a higher spraying power resulted in a thicker alumina layer, whereas an increasing of the power had less effect on the layer formed by the coarser powder.

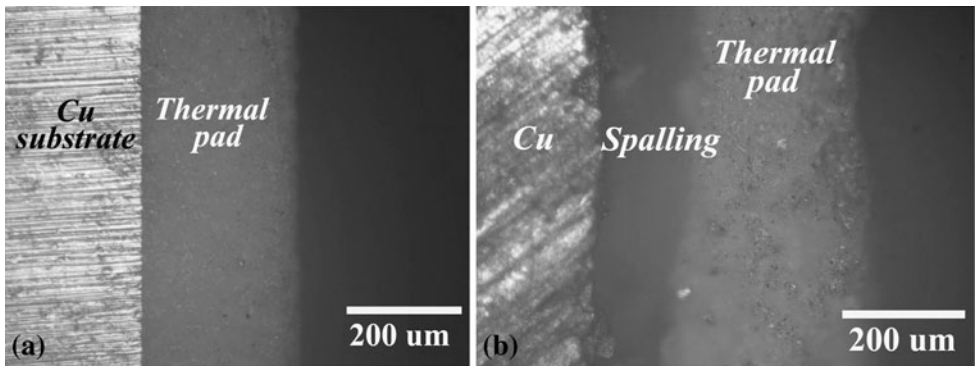

Fig. 3 Optical microscope photographs of specimen S250: (a) before baking and (b) baked at 100 °C for 2 h

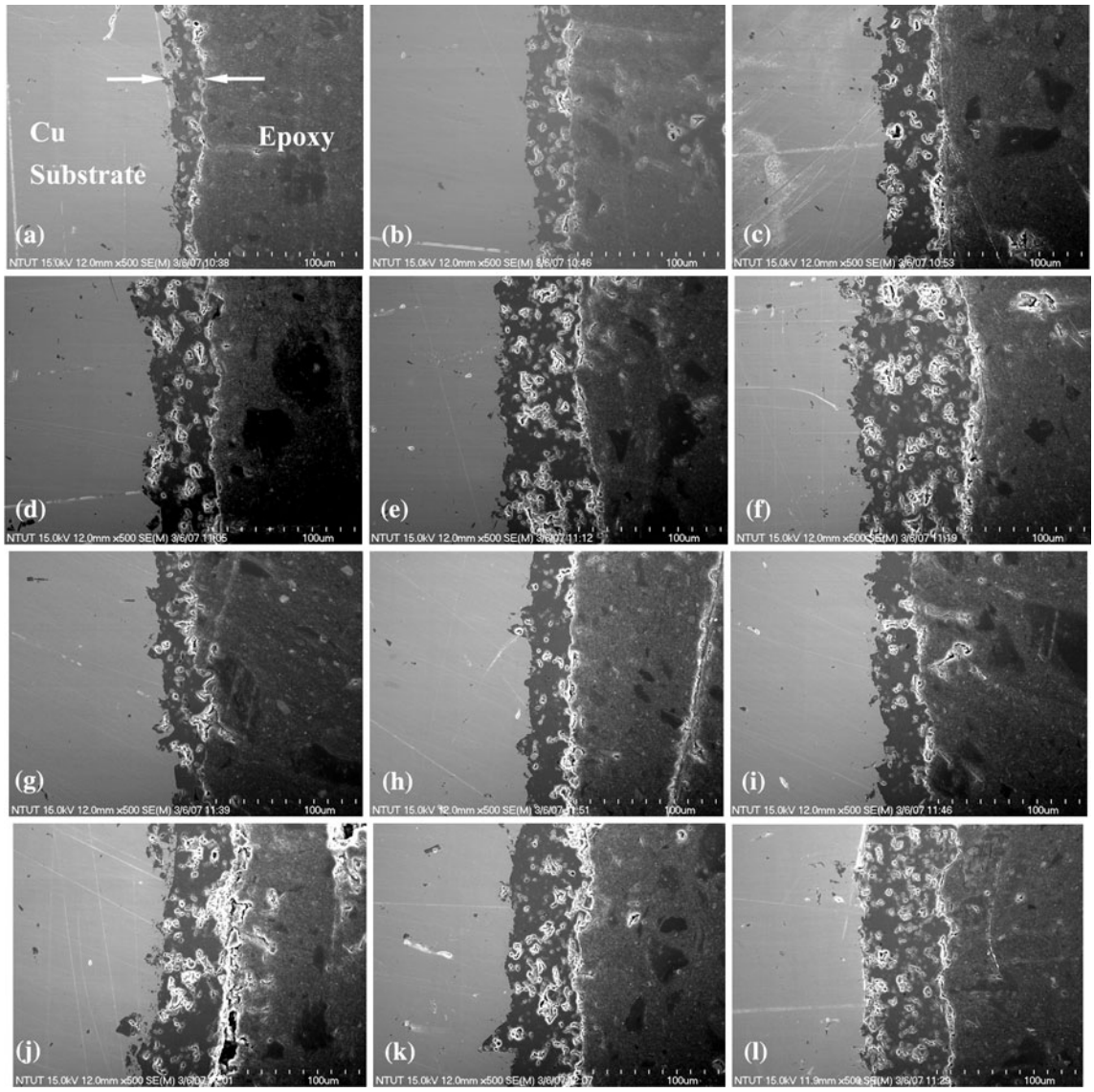

Fig. 4 Secondary electron images of cross-section of plasma spray coating alumina/copper-layered composites, (a) A1, (b) A2, (c) A3, (d) B1, (e) B2, (f) B3, (g) C1, (h) C2, (i) C3, (j) D1, (k) D2, and (l) D3

The EDS mappings of aluminum, copper, and oxygen of specimen C2 (with a layer thickness of 20 μm) are revealed in Fig. 5. Clearly, the composition of the alumina layer was very close to that of the original powder, and no dilution was observed between the alumina layer and the Cu substrate after plasma spray coating.

Figure 6 represents the x-ray diffraction patterns of two groups (A1 to A3 and C1 to C3) alumina/copper specimens with the same layer thickness and alumina particle size, but formed with different plasma spraying power. A comparison with the JCPDS data (Ref 10) indicates that all of the alumina layers were Al_2O_3 phase and the substrate was Cu phase. No new phase formed after plasma spray coating. The crystalline structure of the alumina layer was the same as that of the primitive Al_2O_3 powder.

Figure 7 illustrates the surface roughness (Ra) of all alumina layers formed by plasma spray coating. The mean surface roughness of the specimens in groups A and C was 3.34 and 3.25 μm, respectively. The roughness value of alumina layers in the specimens of group A (particle size of 5-22 μm) is slightly higher than that of group C (particle size of 22-45 μm) by 2.8%. The average surface roughness of the specimens in groups B and D was 3.62 and 3.41 μm, respectively. Similarly, the roughness of the specimens of group B (particle size of 5-22 μm) is also slightly higher than that of group D (particle size of 22-45 μm) by 6.2%. This result reveals that the surface roughness is not only related to the alumina-layered thickness, but also the mass effect of powder. The lower mass of the smaller alumina powder exhibited a relatively lower kinetic energy and enthalpy during plasma spray coating. When alumina particle was injected onto a Cu substrate by plasma spray coating, the smaller alumina particles were cooled down before completely embedded onto the coated layer. Consequently, many pores were formed within the alumina layer and the surface roughness of the coated layer was thus increased. On the other hand, a higher surface roughness of 7.1 μm was reported using a very fine alumina powder, 0.2 μm in diameter (Ref 11), indicating the surface roughness was related to the particle size.

The mean surface roughness of the 40 μm-thick layer (B1 to B3) is slightly higher than that of the 20 μm-thick layer (A1 to

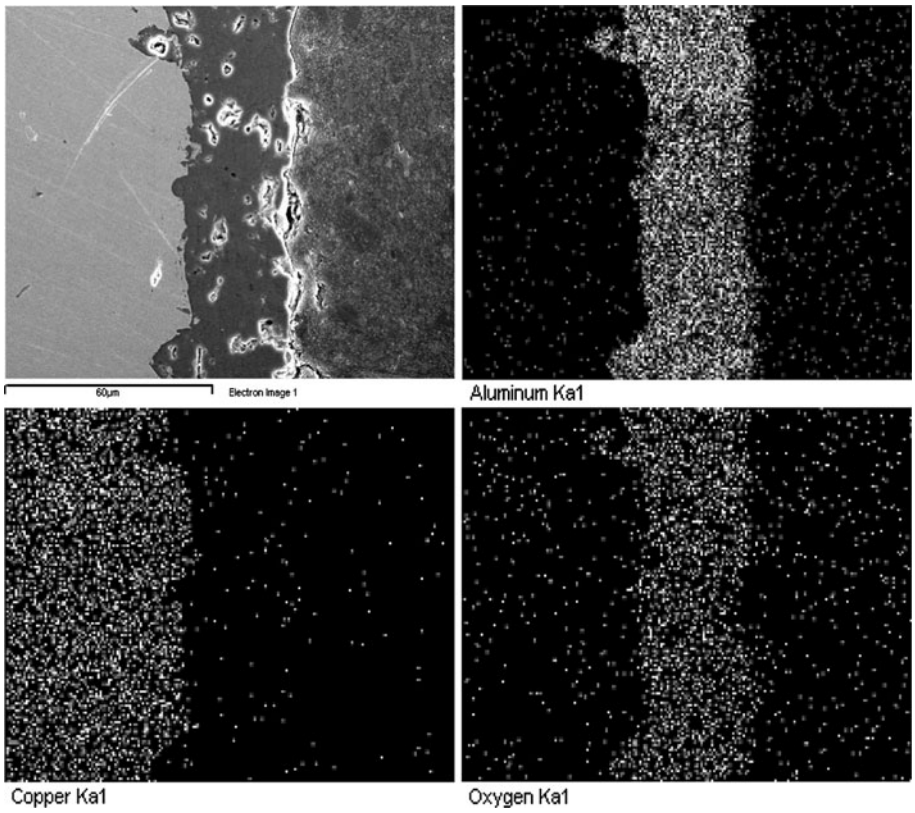

Fig. 5 EDS mapping of aluminum, copper, and oxygen in specimen C2

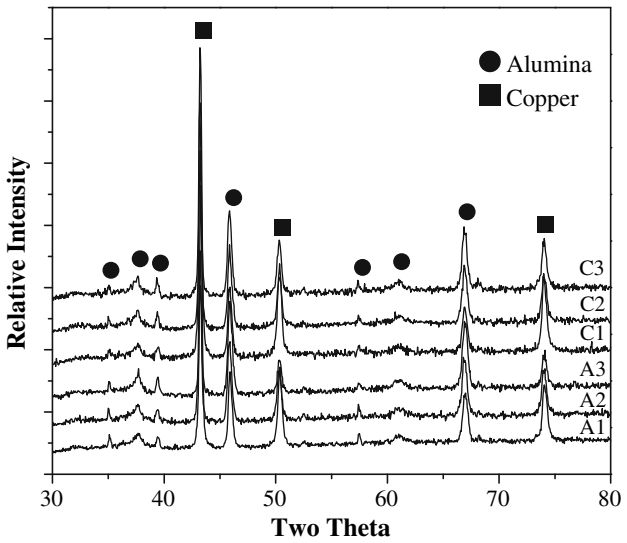

Fig. 6 X-ray diffraction patterns of two groups alumina/copper specimens (with 20 µm-thick layers)

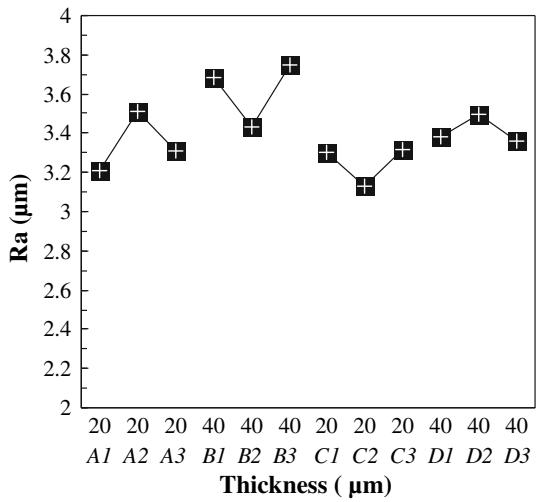

Fig. 7 Surface roughness of all alumina layers of plasma spray coating

A3), even though the alumina particles of the same size were used. The increase in the surface roughness of the alumina layer is caused by the residual stress, which weakens the bonding force between the layer and the substrate. Additionally, the higher porosity of the thicker layer also increases the surface roughness (Ref 12, 13), as presented in Fig. 4(f).

The thermal resistance of each alumina layer formed by plasma spray coating is shown in Fig. 8. The average thermal resistance at an input power of 80 W of specimen groups A, B, C, and D was 0.055, 0.060, 0.042, and 0.045 K/W, respectively.

Figure 9 depicts the surface roughness and thermal resistance of all alumina layers formed by the plasma spray coating. A linear relationship was observed between the surface roughness and the thermal resistance. A comparison between the specimens of group A (with layers of thickness 20 µm) and group B (with layers of thickness 40 µm) reveals that the thermal resistance slightly increases with the layer thickness. However, the average

thermal resistance of group D (0.045 K/W) was almost the same as compared with group C (0.042 K/W), which was possibly attributed to the better surface roughness of each coated layer.

The thermal resistance of the alumina layer specimen C2 was approximately 0.03 K/W, which is nine times less than that of the screen-printed thermal pad (S200, 0.27 K/W). Although pores are easily formed within the plasma spray-coated layer to reduce its thermal conductivity, this process could produce a thinner coated layer around a thickness of 20 μm than the screen-printing process, which yields a layer with a thickness of 200 μm. Consequently, the plasma spray-coated layer had a lower, and more favorable thermal resistance than the screen-printed one.

The thermal resistance of alumina layers formed by plasma spray coating was only 0.03 K/W at a power density of 0.125 W/mm^2, which was equivalent to a thermal conductivity (K) of 3.1 W/m K. These values are superior to those of a PCB, which has a thermal conductivity of 0.3 W/m K (Ref 1). They were also better than those of an IMS, such as a Hitachi-Bergquist substrate on which the insulating layer composed of the epoxy and Al_2O_3 powder with a thermal resistance of 0.35 K/W. Furthermore, a thermal resistance of 0.8 K/W was reported on the Eurolam substrate with an insulating layer consisted of epoxy and glass fibers (Ref 3). In addition, the direct bonding of a dielectric layer and a circuit onto the copper substrate (DBC) yielded a thermal resistance of 0.14 K/W (Ref 5). Apparently, the thermal resistance of the plasma spray-coated alumina layer in this work was five to ten times lower than those of the aforementioned substrates. It is noticed that although the alumina dielectric layer of the MCPCB formed by aerosol deposition had a higher thermal conductivity of 4-5 W/m K (Ref 6), the complicated fabrication processes also yielded a low production rate and high cost.

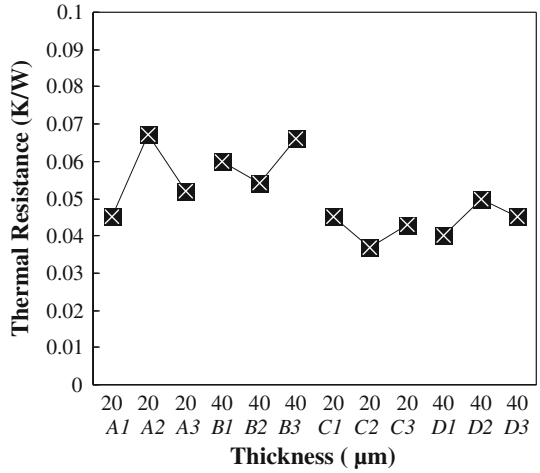

Fig. 8 Thermal resistance of all alumina layers formed by plasma spray coating, over a test area of 0.0254 m × 0.0254 m

All of the alumina dielectric layers formed by plasma spray coating exhibited excellent insulation properties, and the electric resistivity was more than 10^{14} Ω cm, due to the appearance of alumina. In this work, a continuous and uniform layer around 20 μm in thickness was formed using a plasma spray power and alumina particles sizes ranging from 35.2 to 45 kW and 5-45 μm, respectively. The current leakage of the substrate was effectively prevented in this work.

It is reported that the plasma spray coatings tend to be very porous and the porosity around 5-30 vol.% was found (Ref 14). The pores will absorb moisture in a wet and hot environment and thus reduce the breakdown voltage of the alumina dielectric layer. In this work, all specimens were baked at 100 °C for 1 and 2 h, respectively, to compare the breakdown voltages, which are plotted in Fig. 10.

Notably, under the same layer thickness, the breakdown voltage of specimens increases with the plasma spraying power. This phenomenon is caused not only by the improved microstructure, but also by the slightly increased thickness of the layer, which is confirmed by the SEM images shown in Fig. 4(a) and (c). Increasing the thickness of the alumina dielectric layer also increases the breakdown voltage. Such result is very consistent with other investigations (Ref 14, 15). Additionally, the average breakdown voltage of the specimens with a layer thickness of 40 μm (B1 to B3, 50 V/μm) is higher than that of the specimens with a layer thickness of 20 μm (A1 to A3, 38 V/μm) by a factor of around 1.3. The increase in the thickness of the alumina layer did not correspond to the

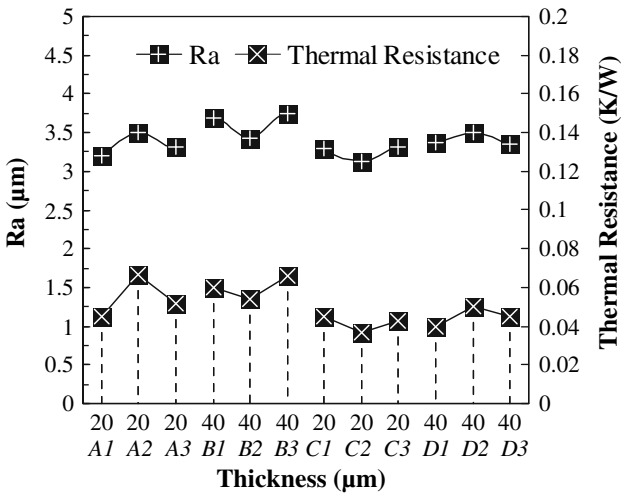

Fig. 9 Surface roughness and thermal resistance of all coated-layers formed by the plasma spray coating

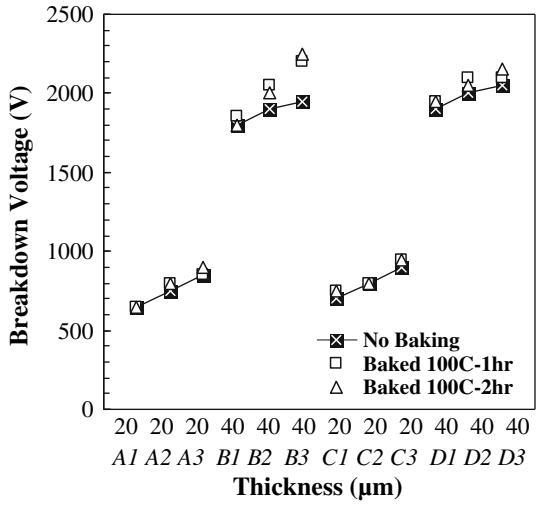

Fig. 10 Breakdown voltage of alumina layer, unbaked, or baked at 100 °C for 1 and 2 h

increase in the breakdown voltage, which may be ascribed to the thinner alumina layer in this work. Hence, a proportional relationship was not observed. If the thickness of alumina layer is more than 100 μm, a positive relationship between the layer thickness and the breakdown voltage will be observed (Ref 15).

On the other hand, baking at 100 °C for 1-2 h increased the mean breakdown voltages of the specimens with a layer thickness of 20 μm (A1 to A3 and C1 to C3) and 40 μm (B1 to B3 and D1 to D3) by 5.1% and 6.0%, respectively. It is noticed that the breakdown voltage of the B3 specimen is increased by over 15%, which is associated with the large number of pores in the thick layer to absorb more moisture than a thin layer. Baking process will remove moisture and therefore increases the breakdown voltage of the alumina layer. This observation is verified by the microstructure of specimen B3, which is presented in Fig. 4(f). In the literature, the breakdown voltage of the MCPCB with a 20 μm-thick alumina layer by the aerosol-deposition of alumina films was 1800 V (90 V/μm) (Ref 6), which was 2.3 times higher than that obtained in this study. It is suggested that the difference is related to the greater porosity formed within the layers during plasma spray coating, since the breakdown voltage of air is lower than that of the alumina layer. As compared with the plasma spray coating in this study, although the breakdown voltage of DBC substrate was around 10,000 V, some disadvantages such as poor thermal shock tolerance caused by the Joule heating of power electronic chips and the brittleness of ceramic during operation were reported (Ref 16). The microstructure and thermal dissipation properties of plasma spray coating and screen-printed alumina on Cu substrate have been explored in this study.

4. Conclusions

It is found that spallation phenomena occur between the alumina thermal pad and the copper substrate of a screen-printed specimen at high temperature, which increased the thermal resistance and reduced the breakdown voltage. On the other hand, the bonding between the alumina layer and the substrate of the plasma spray coating was excellent. The crystal structure and composition of the alumina dielectric layer produced by plasma spray coating were the same as the original alumina powder. It is also observed that smaller alumina particles (5-22 μm) and higher spraying power (45 kW) would form a thicker layer and a higher surface roughness by the plasma spray coating process. The thermal resistance of the alumina layer increased with the surface roughness. The electric insulation of the alumina dielectric layer was excellent, and the electric resistivities of all specimens are higher than 10^{14} Ω cm. In addition, the breakdown voltage of the alumina/copper composite was determined by the thickness and microstructure of the alumina layer, which could be increased slightly by the baking process. In this study, the optimal parameters of plasma spray coating were a plasma power of 40 kW, alumina powder with particle sizes ranging from 22 to 45 μm, an coated alumina layer thickness of 20 μm, a spraying velocity of 750 m/s, an argon flow rate of 45 L/min, a spraying distance of 140 mm, and a spraying angle of 90°.

References

1. T.F. Lemczyk, B. Mack, J.R. Culham, and M.M. Yovanovich, PCB Trace Thermal Analysis and Effective Conductivity, *Proceedings—IEEE Semiconductor Thermal and Temperature Measurement Symposium*, Phoenix, 1991, p 15-22
2. J. Petroski, Spacing of High-Brightness LEDs on Metal Substrate PCB's for Proper Thermal Performance, *Thermomechanical Phenomena in Electronic Systems—Proceedings of the Inter Society Conference*, Vol 2, 2004, p 507-514
3. S.D. Pascoli, P.E. Bagnoli, and C. Casarosa, Thermal Analysis of Insulated Metal Substrates for Automotive Electronic Assemblies, *Microelectron. J.*, 1999, **30**, p 1129–1135
4. S.I. Asai, M. Funaki, H. Sawa, and K. Kato, Fabrication of an Insulated Metal Substrate (IMS), Having an Insulating Layer with a High Dielectric Constant, *IEEE Trans. Comp. Hybrids Manuf. Technol.*, 1993, **16**(5), p 499–504
5. C. Marc, N. James, and A. Robert, Power Modules with IMS Substrates for Automotive Application, *IEEE Vehicular Technology Conference*, Birmingham, Vol 4, 2002, p 2056-2063
6. H.M. Cho and H.J. Kim, Metal-Core Printed Circuit Board with Alumina Layer by Aerosol Deposition Process, *IEEE Electr. Device Lett.*, 2008, **29**(9), p 991–993
7. F. Miyashiro, N. Iwase, A. Tsuge, F. Ueno, M. Nakahashi, and T. Takahashi, High Thermal Conductivity Aluminum Nitride Ceramic Substrates and Packages, *IEEE Trans. Comp. Hybrids Manuf. Technol.*, 1990, **13**(2), p 313–319
8. F. Xiang, H. Wang, M. Zhang, X. Sun, and X. Yao, Preparation and Dielectric Tunability of Bismuth-Based Pyrochlore Dielectric Thick Films on Alumina Substrates, *Ceram. Int.*, 2008, **34**(4), p 925–928
9. M. Darveniza, Electrical Breakdown of Air Between Insulated Conductors, *Proceedings of the IEEE International Conference on Properties and Applications of Dielectric Materials*, Vol 2, 2002, p 615-620
10. JCPDS—International Centre for Diffraction Data, #37-1462, #04-0836, Vol 2.3, 2000
11. Y. Zeng, S.W. Lee, and C.X. Ding, Plasma Spray Coatings in Different Nano-size Alumina, *Mater. Lett.*, 2002, **57**, p 495–501
12. J.S. Reed, *Principles of Ceramics Processing*, John Wiley & Sons, Inc, New York, 1995, p 576–578
13. O. Sarikaya, Effect of Some Parameters on Microstructure and Hardness of Alumina Coatings Prepared by the Air Plasma Spraying Process, *Surf. Coat. Technol.*, 2005, **190**(2–3), p 388–393
14. R. Suryanarayanan, *Plasma Spraying Theory and Applications*, World Scientific Publishing, Singapore, 1993, p 103–114
15. H.J. Kim, S. Odoul, C.H. Lee, and Y.G. Kweon, The Electrical Insulation Behavior and Sealing Effects of Plasma-Sprayed Alumina Titania Coatings, *Surf. Coat. Technol.*, 2001, **140**, p 293–301
16. X.S. Ning, Y. Lin, W. Xu, R. Peng, H. Zhou, and K. Chen, Development of a Directly Bonded Aluminum/Alumina Power Electronic Substrate, *Mater. Sci. Eng. B*, 2003, **99**, p 479–482